Biol. Cybern. 48, 201–211 (1983)

Biological Cybernetics

Lotka-Volterra Equation and Replicator Dynamics: A Two-Dimensional Classification

Immanuel M. Bomze

Institut für Statistik und Informatik, Universität Wien, Austria

Abstract. The replicator equation arises if one equips a certain game theoretical model for the evolution of behaviour in animal conflicts with dynamics. It serves to model many biological processes not only in sociobiology but also in population genetics, mathematical ecology and even in prebiotic evolution. After a short survey of these applications, a complete classification of the two-dimensional phase flows is presented. The methods are also used to obtain a classification of phase portraits of the well-known generalized Lotka-Volterra equation in the plane.

1 Introduction

The introduction of game theoretical concepts into biology by Maynard-Smith and Price (1973) and Maynard-Smith (1974) has provided considerable insight into the problem of altruism in nature and the role of ritual fighting in animal conflicts. To study the evolution of behavioural strategies, the so-called "replicator equation" has been introduced by Taylor and Jonker (1978) and among others has been studied in detail by Hofbauer et al. (1979), Schuster et al. (1980, 1981), and Zeeman (1980, 1981). This replicator equation serves to model not only game dynamics, but also other biological processes occurring in population genetics and even prebiotic evolution; indeed, the "classical" selection equation and the hypercycle equation of Eigen and Schuster (1979) turn out to be special cases of the replicator equation (see Schuster and Sigmund, 1983).

Zeeman (1980) investigated robust flows in the case of three pure strategies. (We shall call a flow or a certain feature of the dynamics "robust", if it remains unchanged under all sufficiently small perturbations; by a "perturbation" we shall understand an alteration of some parameters involved in the model.) He conjectured that no limit cycles exist, which was proved later by Hofbauer (1981) and led to a complete classification of all robust phase portraits (PP's).

However, as the discussion of a four-character game in Zeeman (1981) shows, non-robust properties of the dynamics allow additional interpretations like genetic drift and weak recurrence, so that an investigation of the non-robust cases seems to be of considerable interest.

As Hofbauer (1981) shows, the replicator equation for n strategies corresponds – up to a change in velocity – to the generalized Lotka-Volterra equation for $n-1$ populations. Thus, our problem is equivalent to the classification of the flows of the Lotka-Volterra system on the plane, which was reported by Li (1979) to be contained in his unpublished Ph. D. thesis at the University of Chicago.

From the preceding remarks we see, that the replicator equation together with its equivalent, the Lotka-Volterra equation, covers a wide range of biological modeling in the following fields: sociobiology, population genetics, mathematical ecology and prebiotic evolution.

In Sect. 2, a short survey of the applications of this dynamical model is given by specifying some examples and relating them to the classification which is presented in Sect. 3. The corresponding PP's are listed in Sect. 4. Section 5 indicates how to obtain all 109 PP's of the Lotka-Volterra equation. Finally, Sect. 6 deals with some interrelations among the PP's which may help to group them into classes. The appendix contains some auxiliary results on which the considerations of Sect. 3 are based.

2 Applications and Examples

2.1 Sociobiology: Game Dynamics

Consider an animal population consisting of individuals belonging to the same species. We shall assume that, with respect to a certain type of conflict, the

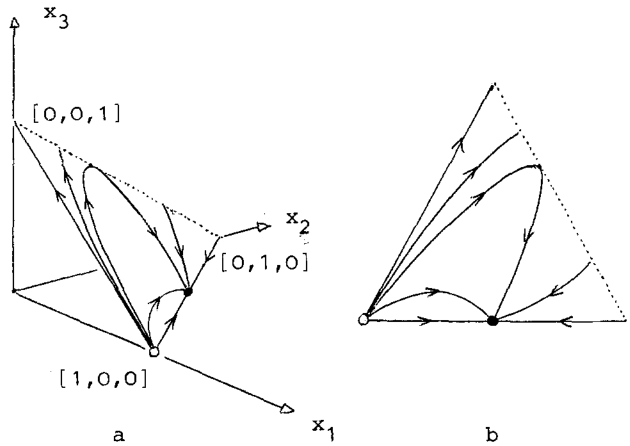

Fig. 1a and b. Phase portrait of the Hawk-Dove-Retaliator game

behaviour of such an individual does not change within its lifetime and is inherited by its offsprings. Let us assume there are n distinct behaviour patterns called "pure strategies", $E_1, E_2, \ldots, E_n$. The state of a population concerning this conflict is fully described by a vector $\mathbf{x}=[x_1, \ldots, x_n] \in \mathbb{R}^n$ where x_i represents the frequency of individuals with behaviour E_i, $i=1, \ldots, n$. Consequently,

$$x_i \geqq 0, \text{ all } i, \quad \text{and} \quad \sum_i x_i = 1.$$

The set of all such x's is denoted by S^n.

If an E_i – individual contends with an E_j – individual, the Darwinian fitness of the former will be altered by the "payoff" a_{ij}. Let A be the matrix consisting of these a_{ij}'s. Assuming random encounters,

$$\mathbf{e}_i \cdot A\mathbf{x} = \sum_j a_{ij} x_j$$

is the average payoff for an E_i – individual in a population $\mathbf{x}$ and

$$\mathbf{x} \cdot A\mathbf{x} = \sum_i x_i \mathbf{e}_i \cdot A\mathbf{x} = \sum_i \sum_j a_{ij} x_i x_j$$

is the mean average payoff within population $\mathbf{x}$. (In Sect. 3 and the appendix, the game theoretical term "mixed strategy $\mathbf{x}$" will be used instead of "population $\mathbf{x}$".)

Following Taylor and Jonker (1978), we assume that the growth rates $\dot{x}_i/x_i = (dx_i/dt)/x_i$ of the frequency of strategy E_i are equal to the payoff difference $\mathbf{e}_i \cdot A\mathbf{x} - \mathbf{x} \cdot A\mathbf{x}$. This yields the replicator equation

$$\dot{x}_i = x_i[\mathbf{e}_i \cdot A\mathbf{x} - \mathbf{x} \cdot A\mathbf{x}] \qquad i=1, \ldots, n \tag{1}$$

on the invariant set S^n.

As an example for deriving the payoff-matrix from a "live-scenario", consider the well-known Hawk-Dove-Retaliator game by Maynard-Smith and Price (1973) (see also Maynard-Smith, 1982), where animals are contesting a ressource of value $V>0$:

The pure strategy E_1 ("Hawk") represents an escalating behaviour; escalation will be continued until injury (which costs $C>0$) or retreat of the opponent.

The strategy E_2 ("Dove") consists of displaying in a ritual way. A Dove retreats if opponent escalates.

Strategy E_3 ("Retaliator") behaves like a Dove against a Dove and like a Hawk against a Hawk but never escalates first.

We shall assume that each of the two escalating opponents have a 50% chance of injuring the other one and obtaining the ressource, and a 50% chance of being injured; similarly, two displaying contestants shall have a 50% chance of "winning" the ressource. Now it is easy to derive A:

$$A = \begin{bmatrix} \frac{V-C}{2} & V & \frac{V-C}{2} \\ 0 & V/2 & V/2 \\ \frac{V-C}{2} & V/2 & V/2 \end{bmatrix}.$$

For example, $V=2$, $C=4$; then

$$A = \begin{bmatrix} -1 & 2 & -1 \\ 0 & 1 & 1 \\ -1 & 1 & 1 \end{bmatrix}$$

yields a flow on S^3 (for brevity, set $S=S^3$) depicted in Fig. 1a. Figure 1b shows a more practicable view on S which we will use from now on (cf. Subsect. 3.3 and the rotated PP [23] in Fig. 6).

Let us discuss Fig. 1b in detail: the corners represent populations consisting only of Hawks, Doves, Retaliators, respectively. The point [1, 0, 0] (only Hawks) is a "source", i.e. all populations with (sufficiently) small amounts of Doves and Retaliators will evolve away from [1, 0, 0], which means that the frequencies of Doves and Retaliators will increase. The point [1/2, 1/2, 0] which represents a 50% mixture of Hawks and Doves in the absence of Retaliators is a "sink", i.e. all populations with small amounts of Retaliators and a Hawk-Dove ratio close to 1, will evolve towards [1/2, 1/2, 0]. In this case Retaliators will become extinct and there will remain an equal number of Doves and Hawks.

Sources and sinks are given by linearization and describe the flow only in a neighbourhood of the fixed point. We are interested in a global picture of the flow. Further analysis will show (see Subsect. 3.3) that any mixed population will evolve according to its initial condition: either to a population with no Hawks and twice as many Doves as Retaliators at the most, or to the above mentioned 1:1-mixture of Hawks and

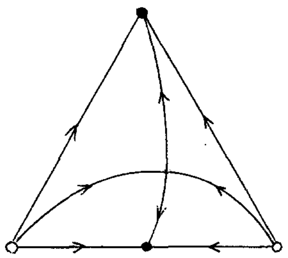

Fig. 2. Phase portrait of the "robustified" Hawk-Dove-Retaliator game

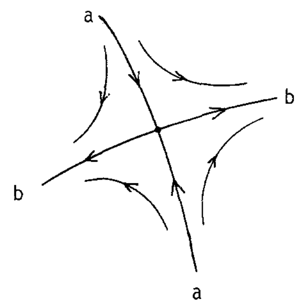

Fig. 3. Flow in a neighbourhood of a saddle point "*a*": inset, "*b*": outset of the saddle point

Doves. If in a population Doves are absent, Hawks will die out; if Hawks are missing, nothing will happen: the population corresponds to a fixed point. If there are no Retaliators, Hawks and Doves will become equally frequent. The arrows in Fig. 1 shall indicate the evolution described above.

This PP is an example for that of a non-robust flow (whenever there are infinitely many fixed points, the flow is non-robust). Indeed, let us slightly alter some of the a_{ij}'s: consider a small advantage of Retaliators against Doves (as suggested by Zeeman, 1981) yielding

$$A=\begin{bmatrix}-1 & 2 & -1\\ 0 & 1 & 1-\varepsilon\\ -1 & 1+\varepsilon & 1\end{bmatrix}, \quad \varepsilon>0, \text{ small}.$$

Figure 2 shows the corresponding PP (cf. [14] in Fig. 6); again, [1, 0, 0] is a source and [1/2, 1/2, 0] a sink. But now, [0, 1, 0] (only Doves) is another source and [0, 0, 1] (only Retaliators) another sink. In addition to these, there is another fixed point in the interior of S which is neither a source nor a sink but a so-called "saddle point" in whose neighbourhood the flow looks like in Fig. 3.

Thus, every population (except the mentioned fixed points and except the points on trajectories joining the saddle point with sources and sinks, the "in-" and "outsets", cf. Fig. 3), evolves according to its initial state: either towards a 1:1-mixture of Hawks and Doves without Retaliators, or to a pure Retaliator population. If Doves or Retaliators are absent, the same happens as in the game discussed above; but if Hawks are missing, Doves will, contrary to the former model, die out.

2.2 Population Genetics: Selection as a Game of Partnership

In a game of partnership, the two contestants share their outcome equally which means $a_{ij}=a_{ji}$, all i and j. If x_i, $i=1,\dots,n$, are the frequencies of n possible alleles for a given chromosomal locus and a_{ij} is the fitness of genotype (ij), (1) is the well-known Wright-Fisher-Haldane model continuous in time in population genetics (cf. Hadeler, 1974). The mean average payoff (=fitness) $\mathbf{x}\cdot A\mathbf{x}$ increases with time and every population approaches some fixed point (Akin and Hofbauer, 1982). For example, consider a three-alleles model where heterozygotes are fitter than homozygotes:

$$A=\begin{bmatrix}1 & 2 & 2\\ 2 & 1 & 2\\ 2 & 2 & 1\end{bmatrix}.$$

This leads to PP [7] in Fig. 6; a population consisting initially of all three types of genes will converge to the sink in the middle of S. Other examples of selection PP's are [1], [20], [22], [34], and [35] in Fig. 6.

2.3 Prebiotic Evolution: The Hypercycle

The simplest possible hypercycle model is that of three species 1, 2, 3 of interacting macromolecules with concentrations x_1, x_2, x_3, respectively. Let us assume, that by a catalytic mechanism species 2 favours growth of species 1 which in turn favours species 3, which again favours species 2. As is shown in Schuster and Sigmund (1983), Eq. (1) describes the evolution of this model if one sets

$$A=\begin{bmatrix}0 & k_1 & 0\\ 0 & 0 & k_2\\ k_3 & 0 & 0\end{bmatrix}, \quad k_i>0, \text{ all } i.$$

The PP is depicted as [17] in Fig. 6: every population approaches the interior sink, cooperation results. Despite the fact that in both PP's [7] and [17] are interior sinks, there is a significant distinction between them: while in the first case all frequencies increase or decrease monotonically, in the second the frequencies oscillate. In the PP's this difference is manifested by approaching the fixed point in [7] along an almost straight line while spiraling towards it in [17].

2.4 Mathematical Ecology: The Lotka-Volterra Equation

Consider two interacting populations with densities $x(\geqq 0)$ and $y(\geqq 0)$. The simplest formal description of interaction is a dynamical system with linear dependence of the growth rates $\dot{x}/x$ and $\dot{y}/y$ on the densities. This yields

$$\left.\begin{aligned}\dot{x}&=x[a+bx+cy]\\ \dot{y}&=y[d+ex+fy]\end{aligned}\right\} \tag{2}$$

which represents the general Lotka-Volterra equation in the plane or, more precisely, in the positive quadrant

$$\mathbb{R}^2_+=\{[x,y]\in\mathbb{R}^2: x\geqq 0, y\geqq 0\}.$$

The signs of b, c, e, f represent growth enhancing (if positive), indifference (if zero) or inhibiting effect (if negative) of one species upon itself or the other one. Again, the terms x^2, xy, y^2 may be viewed as caused by random encounters.

If we set for $[x,y]\in\mathbb{R}^2_+$

$$x_1=\frac{1}{1+x+y},\quad x_2=\frac{x}{1+x+y},\quad x_3=\frac{y}{1+x+y} \tag{3}$$

then it is obvious that $[x_1, x_2, x_3]\in S$. Hofbauer (1981) applied this transformation to show that (2) is equivalent to (1) with matrix

$$A=\begin{bmatrix}0&0&0\\a&b&c\\d&e&f\end{bmatrix}. \tag{4}$$

But at first let us turn to applications and important cases of (2). Since they all are well-known, we briefly describe the resulting PP's by referring to the corresponding PP of (1). See Sect. 5 for constructing PP's of (2) from PP's of (1).

2.4.1 Predator-Prey Models. In this case, the corresponding PP's of (1) are $\boxed{9}$, $\boxed{15}$, $\boxed{16}$, $\boxed{37}$, $\boxed{39}$, $\boxed{41}$, and $\boxed{42}$ in Fig. 6 up to suitable geometric transformations. So one has to reflect PP's $\boxed{15}$ and $\boxed{41}$ such that left- and right-hand corners are interchanged, $\boxed{9}$ and $\boxed{37}$ such that above and right-hand corners are interchanged, and to rotate PP $\boxed{39}$ before proceeding as in Sect. 5. The counterpart of $\boxed{16}$ consists of an interior fixed point, the predator-prey equilibrium, and closed orbits surrounding it which represent endless periodic oscillations. This is the PP of the classical predator-prey model developed independently by Lotka and Volterra. All other PP's occur if one introduces intraspecific competition and fall into two classes: in the analogous cases to $\boxed{37}$, $\boxed{39}$, $\boxed{41}$, and $\boxed{42}$, predators will vanish and the prey population approaches a limiting value which is stricly positive and finite. The differences between the above mentioned PP's concern only the past (as $t\to-\infty$).

In the second class, consisting of the pendants to $\boxed{9}$ and $\boxed{15}$, there is an interior sink and a saddle point representing a pure prey population. This means that almost every population evolves towards the predator-prey equilibrium: coexistence will be established.

2.4.2 Competition Models. Competition models of the form (2) arise if one assumes that ressources decrease linearly with the population densities of two competing species and that the growth rates increase linearly with the ressources. The corresponding PP's are to obtain from $\boxed{1}$, $\boxed{5}$, $\boxed{7}$, $\boxed{8}$, $\boxed{9}$, $\boxed{10}$, $\boxed{21}$, $\boxed{34}$, $\boxed{35}$, $\boxed{37}$, $\boxed{38}$ in Fig. 6 after suitable geometric transformations. The last five cases represent extinction of one species and occur, for instance, if only one (the one for which both species compete) ressource is present; this fact is often called "exclusion principle". That this principle does not hold in all competition models is shown by the counterparts to $\boxed{7}$ and $\boxed{9}$ where the interior sink represents coexistence of both species. $\boxed{8}$ and $\boxed{10}$ correspond to situations where one, or the other of both populations will vanish depending on their initial conditions. In the non-robust cases corresponding to $\boxed{1}$, $\boxed{5}$, all orbits converge to a pointwise fixed straight line which means that an equilibrium between both species is reached. This equilibrium depends on the initial states of the populations. In the one-ressource case, these flows are the only non-robust ones. Since random fluctuations along the line of fixed points may cause extinction of one species, one may say, that the exclusion principle in a generalized meaning is still valid.

3 Classification

This section is based on the propositions and corollaries of the appendix which are numbered from 1 to 9. Let us introduce some useful notions:

By an "eigenvalue (EV) of a fixed point" we shall understand an eigenvalue of the linearization matrix (not A) around that fixed point. The term "EV in direction of $\mathbf{v}$", $\mathbf{v}$ a vector or a ray, means that $\mathbf{v}$ is an eigenvector of the linearization matrix corresponding to that EV. A fixed point is called "hyperbolic" if its EV's have non-vanishing real parts.

Let $k_1=\{[x,0]: x>0\}$, $k_2=\{[0,y]: y>0\}$ be the boundary rays of $\mathbb{R}^2_+$ and $\operatorname{Int} S=\{\mathbf{x}\in S: x_i>0 \text{ for all } i\}$ denote the set of mixed strategies where every pure strategy is involved. An "edge" of S consists of all mixed strategies which do not involve a (fix) pure strategy. Thus, S is the union of $\operatorname{Int} S$ and its three edges.

It seems reasonable to distinguish at first cases according to the number of fixed points in Int$S$.

Case 0: More than two fixed points in Int$S$, not all on one straight line.

Case I: More than one fixed point in Int$S$, all on one straight line.

Case II: Exactly one fixed point in Int$S$.

Case III: No fixed point in Int$S$.

3.1 More than One Fixed Point in Int$S$

Case 0: Proposition 9 and the following remark show $A=[0]$: PP [0].

Case I: According to Proposition 6, there is a pointwise fixed straight line g which does not coincide with k_1 nor k_2. Proposition 2 shows that in this case not both k_1 and k_2 can be pointwise fixed (otherwise one would have $A=[0]$), whence two different subcases arise:

I.a There is exactly one edge which is pointwise fixed.

I.b There is no pointwise fixed edge.

I.a: Let $\bar{g}$ denote the pointwise fixed straight line under (1) – such that $\bar{g}\cap\text{Int}S$ is a segment – and k the pointwise fixed edge of S. Then there are three cases:

I.a.1 $k\cap\bar{g}=\emptyset$,

I.a.2 $k\cap\bar{g}=\{\mathbf{e}_i\}$, $\mathbf{e}_i$ a corner,

I.a.3 $k\cap\bar{g}=\{\mathbf{p}\}$, $\mathbf{p}$ no corner.

In any case there is an edge $k'\neq k$ of S which intersects $\bar{g}$. If we now assume without loss of generality that k_1, k_2 correspond to k, k', respectively, we obtain up to geometric equivalence (i.e. reflections, rotations) and/or flow reversal four different PP's of (2) from which the PP's [1], [2], [3], [4] of (1) are derived: I.a.1 corresponds to [1], I.a.2 to [2] and I.a.3 to [3] and [4]. Later on, we will also identify PP's of (1) in which the flow has the same limit behaviour irrespective of differential geometric differences (e.g. in curvature etc.).

I.b: A short reasoning shows that no corner of S can lie on $\bar{g}$, otherwise one would obtain a contradiction by Propositions 2 and 6(i). Hence there are two edges with an isolated non-vertex fixed point and the only possible PP's are [5] and [6].

3.2 One Fixed Point in Int$S$

It follows from Propositions 2 and 6(ii) that no edge can be pointwise fixed; this yields the distinction

II.a three non-corner fixed points on edges,

II.b two non-corner fixed points on edges,

II.c one non-corner fixed point on an edge,

II.d no non-corner fixed point on an edge.

II.a: Corollaries 3, 4 and 8 show that all fixed points on the edges are hyperbolic; from Propositions 2 and 5 we can infer that

$$ab<0, \quad df<0 \quad \text{and} \quad (e-b)(f-c)<0,$$

whence it follows by Corollary 7(ii) that if $bf<ce$, all fixed points are hyperbolic, while if $bf>ce$ a short argument via Proposition 6(ii) shows that $bf>0$; hence $\text{sign}(bp+fq)=\text{sign}(b)\neq 0$ which means [Corollary 7(iii)!] that all fixed points are hyperbolic (recall that by Proposition 6, $bf\neq ce$!).

Since there are no limit cycles (see Hofbauer, 1981), only the robust PP's [7] and [8] can occur.

II.b: Similar reasoning as above shows that in the case $bp\neq -fq$ the interior fixed point is hyperbolic (use Proposition 6 and Corollary 7).

Since only one EV of fixed points on edges can vanish (e.g. $e=b$ or $f=c$), only robust flows on the edges are possible so that only one non-robust PP can occur which was already given in Zeeman (1980). Thus one obtains the PP's [9] to [13].

II.c: In this case, no non-robust PP's can occur since $bp+fq\neq 0$ (using an argument analogous to that in II.b). This leads to the robust PP's [14] and [15].

II.d: Again there are but robust flows on the edges whence it follows that the only non-robust case is $bf>ce$, $bp+fq=0$, which is covered already by Hofbauer (1981) and Zeeman (1980) and has PP [16]; the robust PP is [17].

3.3 No Fixed Point in Int$S$

If all edges were pointwise fixed, Propositions 2 and 5 would yield $A=[0]$. Thus we have only to distinguish between

III.a two edges pointwise fixed,

III.b one edge pointwise fixed,

III.c no edge pointwise fixed.

III.a: The trajectories are straight lines: indeed, assume without loss of generality that k_1 and k_2 are pointwise fixed. Proposition 2 then yields

$$cy(t)=K+ex(t).$$

Thus one has the PP's [18], [19], and [20].

III.b: There are the following cases:

III.b.1 two isolated non-corner fixed points on edges,

III.b.2 one isolated non-corner fixed point on an edge,

III.b.3 no isolated non-corner fixed point on an edge.

If we assume without loss of generality that k_1 is pointwise fixed and exclude the case $c=0$ (which yields PP [29]), we have to solve the differential equation

$$cxy'=fy+d+ex \tag{5}$$

which gives the PP's [21] and [22] for III.b.1, [23] to [29] for III.b.2 and [30] to [33] for III.b.3 according to the relations between the parameters c, d, e, f.

As an example for that procedure we consider the case III.b.1: according to Propositions 2 and 5 we have $a=b=0$, $df<0$, $e(f-c)<0$. The general solution of (5)

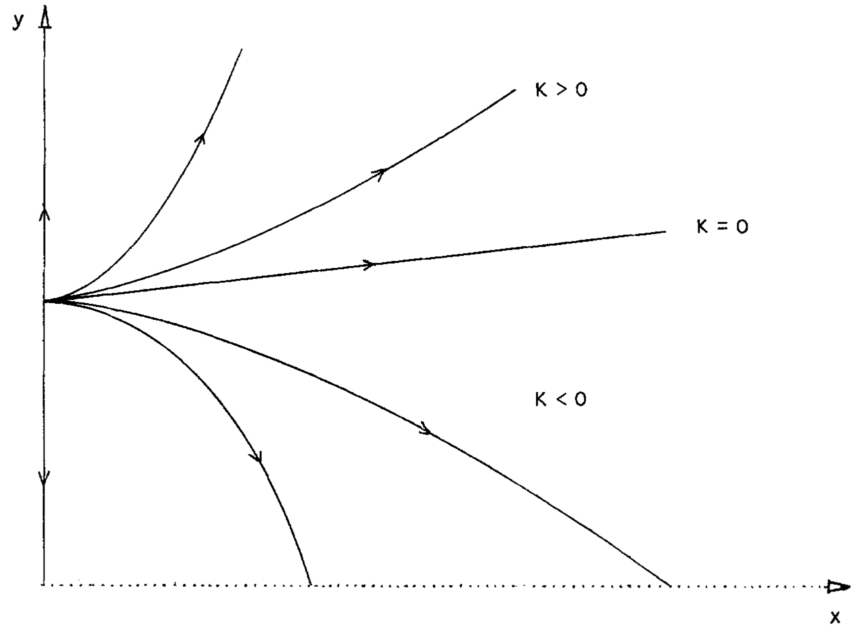

Fig. 4. Integral curves of (5) in the case of $f>c>0$, $d<0$, $e<0$

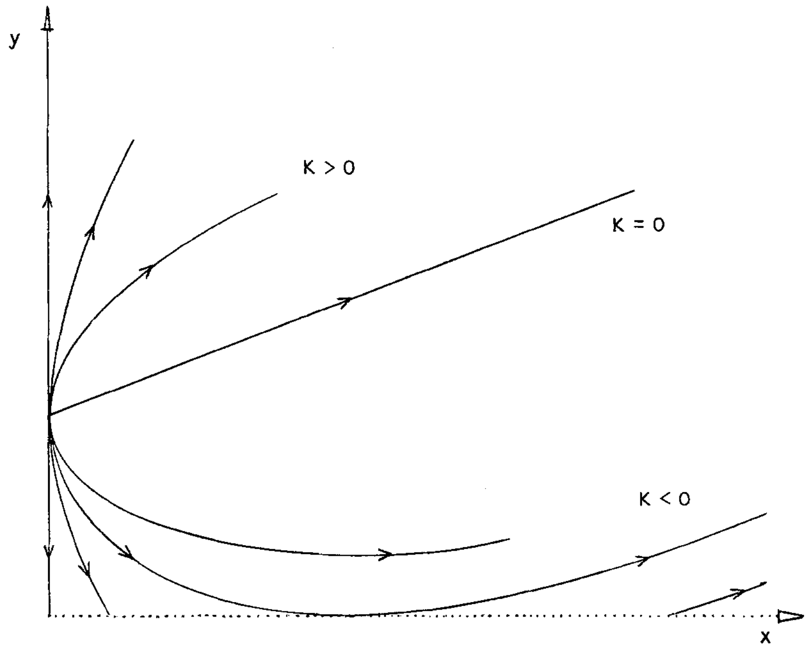

Fig. 5. Integral curves of (5) in the case of $c>f>0$, $d<0$, $e<0$

is then

$$y(x)=Kx^{f/c}+\frac{e}{c-f}x-\frac{d}{f}.$$

Thus one obtains for $f>c>0$ Fig. 4, which yields [21]; the cases $f<c<0$, $f>0>c$, $f<0<c$ are up to flow reversal and/or geometric equivalence the same. But if $c>f>0$ (or $c<f<0$: flow reversal!), then Fig. 5 and PP [22] results.

III.c: From Propositions 1, 2, and 5 we can deduce that on every edge there is at least one corner which has a non-vanishing EV in direction of that edge, whence we can infer that only robust flows on the edges occur.

As a consequence of Poincaré-Bendixson theory, the only possible robust PP's are [34] to [43]. Non-robust subcases of III.c can only occur if both EV's of (exactly) one corner vanish, e.g. $a=d=0$ as EV's of $[0,0]$.

Let

$$g_1=\{[x,y]\in\mathbb{R}_+^2: bx+cy=0\},$$
$$g_2=\{[x,y]\in\mathbb{R}_+^2: ex+fy=0\},$$
$$g_3=\{[x,y]\in\mathbb{R}_+^2: (b-e)x+(c-f)y=0\}.$$

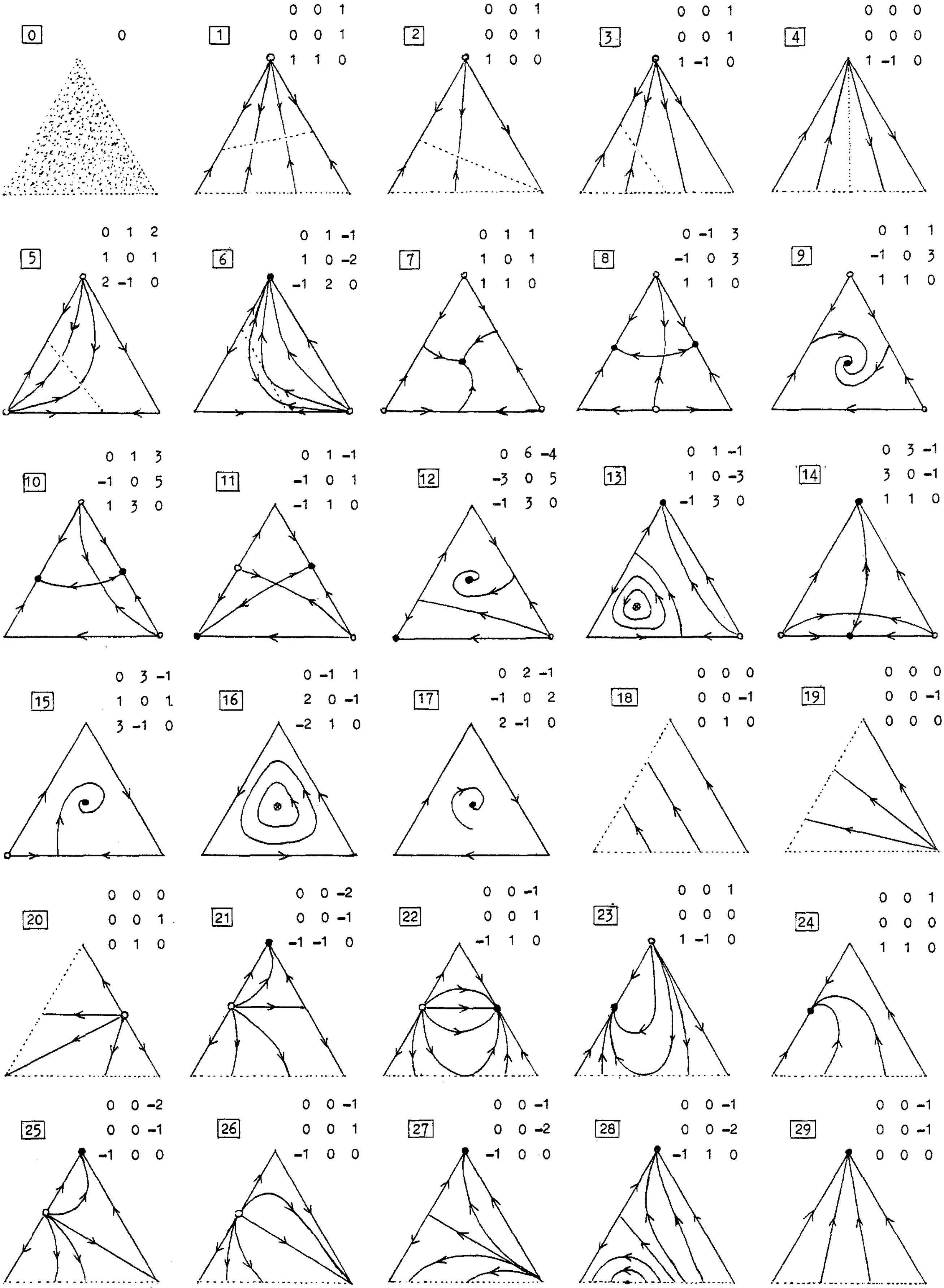
0
0
1
0 0 1
0 0 1
1 1 0
2
0 0 1
0 0 1
1 0 0
3
0 0 1
0 0 1
1 -1 0
4
0 0 0
0 0 0
1 -1 0
5
0 1 2
1 0 1
2 -1 0
6
0 1 -1
1 0 -2
-1 2 0
7
0 1 1
1 0 1
1 1 0
8
0 -1 3
-1 0 3
1 1 0
9
0 1 1
-1 0 3
1 1 0
10
0 1 3
-1 0 5
1 3 0
11
0 1 -1
-1 0 1
-1 1 0
12
0 6 -4
-3 0 5
-1 3 0
13
0 1 -1
1 0 -3
-1 3 0
14
0 3 -1
3 0 -1
1 1 0
15
0 3 -1
1 0 1
3 -1 0
16
0 -1 1
2 0 -1
-2 1 0
17
0 2 -1
-1 0 2
2 -1 0
18
0 0 0
0 0 -1
0 1 0
19
0 0 0
0 0 -1
0 0 0
20
0 0 0
0 0 1
0 1 0
21
0 0 -2
0 0 -1
-1 -1 0
22
0 0 -1
0 0 1
-1 1 0
23
0 0 1
0 0 0
1 -1 0
24
0 0 1
0 0 0
1 1 0
25
0 0 -2
0 0 -1
-1 0 0
26
0 0 -1
0 0 1
-1 0 0
27
0 0 -1
0 0 -2
-1 0 0
28
0 0 -1
0 0 -2
-1 1 0
29
0 0 -1
0 0 -1
0 0 0

Fig. 6 [0] — [29]

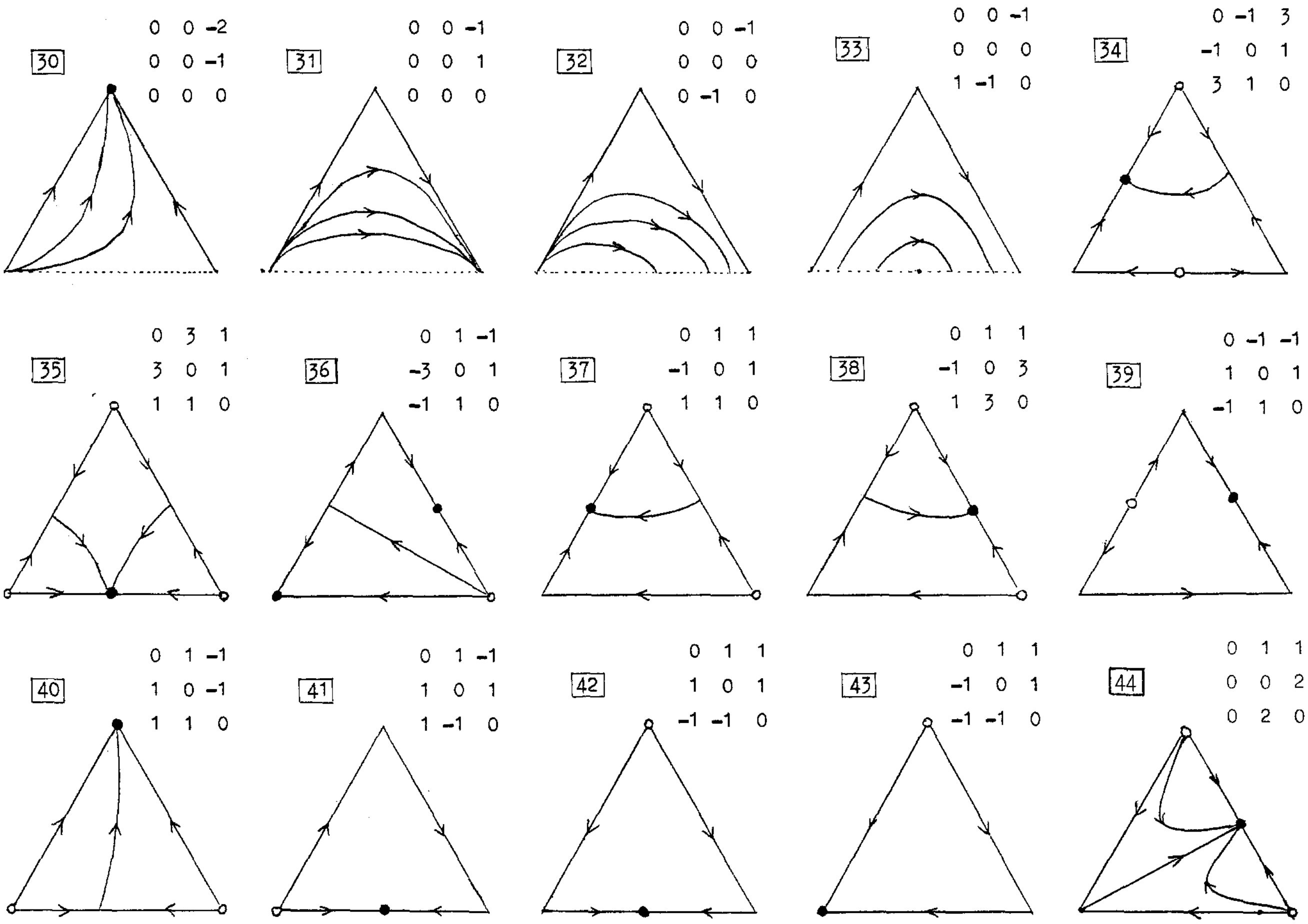

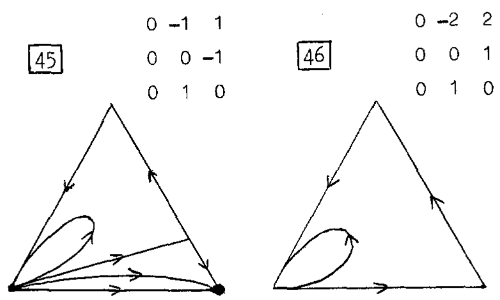

Fig. 6 30 — 46

Fig. 6. The phase portraits of the replicator equation (1)

It is easy to see that g_3 represents a solution curve of (2), an orbit. The only interesting case is

$0 < \text{slope}(g_1) < \text{slope}(g_2)$,

since in all other cases $[0, 0]$ is either a source, a sink or a saddle point which yields one of the PP's 34 to 43.

Now either

$\text{slope}(g_1) < \text{slope}(g_3) < \text{slope}(g_2)$

or

$0 < \text{slope}(g_3) < \text{slope}(g_1)$

(symmetrically, $\text{slope}(g_2) < \text{slope}(g_3)$)

or

$\text{slope}(g_3) \leq 0$

or

g_3 is vertical.

[By virtue of Proposition 6(i), $g_3 = g_1$ if and only if (iff) $g_1 = g_2$ iff $g_2 = g_3$; in this case, $g_1 = g_2 = g_3$ is a pointwise fixed straight line, see I.]

Thus one obtains the PP's 44, 45, and 46.

4 The Phase Portraits of the Replicator Equation

The PP's 0 to 46 were listed in Fig. 6; sources are represented by open dots (○), sinks by full dots (●), centres by crossed dots (⊗), and saddle-points by their insets and outsets (stable and unstable manifolds). In the robust cases (except 17, where every nonconstant

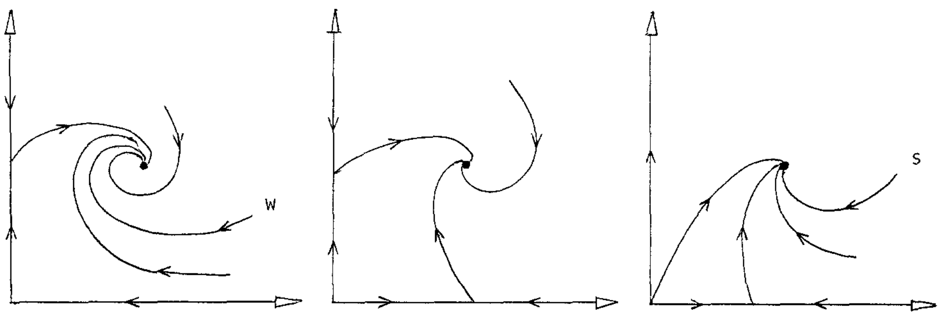

Fig. 7. The phase portraits of the Lotka-Volterra equation (2) corresponding to [9] in Fig. 6

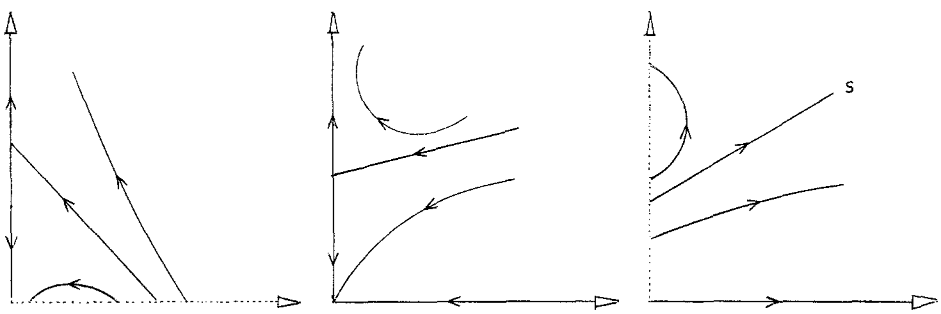

Fig. 8. The phase portraits of the Lotka-Volterra equation (2) corresponding to [28] in Fig. 6

orbit approaches any point on the edges infinitely often), i.e. [7] to [12], [14], [15], [34] to [43], every orbit not specified flows from a source to a sink. In all other cases, some representative orbits are drawn. To each PP a typical matrix A of the form (6) (see appendix) is attached.

5 Classification of the Lotka-Volterra Dynamic

If we reverse the transformation

$$T:[x_1,x_2,x_3]\mapsto[x,y]=\left[\frac{x_2}{x_1},\frac{x_3}{x_1}\right],\quad \text{i.e. consider}$$

$$T^{-1}:[x,y]\mapsto[x_1,x_2,x_3]=\left[\frac{1}{1+x+y},\frac{x}{1+x+y},\frac{y}{1+x+y}\right],$$

then it is clear that we can easily obtain all possible PP's of (2) by "projecting" (in the sense of affine geometry) the PP's [0] to [46] from the corners.

Take, for instance, PP [9]: if we project from the left-hand, above, or right-hand corner, respectively, we obtain the PP's of (2) given in Fig. 7. As another example, consider PP [28] of (1); the corresponding PP's of (2) are depicted in Fig. 8. In both figures, an "s" denotes a trajectory which separates orbits with different limit behaviour (finite/infinite) as $t\to-\infty$ or $t\to+\infty$ while a "w" denotes the orbit which separates trajectories that all tend to infinity but possess different asymptotic behaviour (limit of slope of tangent) as $t\to-\infty$ or $t\to+\infty$.

"w" and "s" trajectories correspond to the insets resp. outsets flowing to resp. coming from saddle points in PP's of (1).

Proceeding in this manner for all 47 PP's of the replicator equation (1), one obtains 109 different PP's of the Lotka-Volterra equation (2) up to flow reversal and/or geometric equivalence. For a complete list of them is of course not enough space here, but it may be interesting to note that there are 42 robust and 67 non-robust PP's of (2) while there are 19 robust and 28 non-robust PP's of (1).

6 On Related Phase Portraits

In this section, with the help of some examples, hints are given how to take non-robust PP's for limiting cases of robust ones and, more generally, to find some relations between the PP's.

If we consider, for instance, [1], [2], [3], and [4] of Fig. 6 in this order, we can easily imagine how the pointwise fixed straight line "wanders". Similarly, if we reverse the flow of [16] which means that all orbits flow clockwise oriented now, denote the corresponding PP −[16], then consider a flow-reversed and reflected PP [17],−[17]′, (one can obtain −[17]′ from [17] simply by substituting a source for the interior sink), −[16] can be viewed as a limiting case between −[17]′ and [17] [see Fig. 9 and Zeeman (1980)].

In the situation of [12] and [13], interchange at first left-hand and above corners in [12] (to obtain [12]′) and

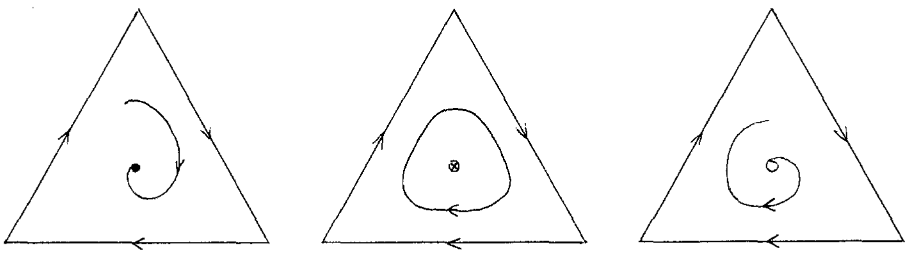

Fig. 9. A non-robust phase portrait as a limiting case between two robust ones

then let in [13] the saddle point in the interior of the bottom edge converge against the right-hand corner. Then, as before, closed orbits become spiraling ones and thus [13] is a limiting case of [12]'. Furthermore, if in [38] the left-hand corner and the saddle point on the left-hand edge coincide, we have [44]; if in [39] source and sink unite in the above corner, one obtains the rotated PP of [46].

As an example for relations between two robust PP's let the sink in the bottom edge of [41] wander into Int$S$; then a saddle point is "left" (more precisely, it originates,) and we obtain PP [15]. Or, if the saddle point on the left- and right-hand edge in [9] are shifting towards the above and right-hand corner, respectively, PP [17] results.

Finally, it may be worth noticing that there are non-robust matrices which can induce a robust flow. (A matrix A is called "robust" if the inequalities between its entries a_{ij} that are relevant for classification are strictly valid; some of these relevant inequalities are specified in Sect. 3.) For instance, the evidently non-robust matrix appearing in the hypercycle equation (cf. Subsect. 2.3) yields the robust PP [17]. A robust matrix A yielding the same is specified in Fig. 6.

7 Conclusions

After a short survey of their applications, we investigated and classified completely the phase portraits of two dynamical systems used in biomathematics: the replicator equation in the case of three pure strategies and the Lotka-Volterra equation on the plane. While the dynamics of the former has the advantage to leave the compact set S invariant, the latter operates on the positive quadrant $\mathbb{R}^2_+$ and is of the simpler analytic form. Hofbauer's transform T enabled us to "switch" between the two dynamics in order to exploit the advantageous features of either systems. By distinguishing cases according to the fixed point structure (i.e. number, position, stability properties of fixed points) we obtained 47 essentially different phase portraits of the replicator equaution and 109 phase portraits of the Lotka-Volterra dynamics.

Acknowledgements. I wish to thank Prof. Dr. Karl Sigmund and Dr. Josef Hofbauer for many stimulating discussions. This work has been finished while the author received financial support for scientific purposes by the Austrian Bundesministerium für Wissenschaft und Forschung.

Appendix

Without loss of generality one can assume A to be of the form (4). Indeed, adding a constant to each column of A does not change the dynamics given by (1); the same effect like (4) yields, for instance,

$$A=\begin{bmatrix} 0 & -b & -f \\ a & 0 & c-f \\ d & e-b & 0 \end{bmatrix}. \tag{6}$$

In Sect. 4, the representative matrices are of the type (6).

The transformation T specified in Sect. 5 maps the set of all mixed strategies where E_1 is involved with a positive probability, i.e. $\{\mathbf{x}\in S: x_1>0\}$ to the positive quadrant $\mathbb{R}^2_+$.

With these facts in mind, one obtains easily

Proposition 1. *The* EV's *of the corners representing* E_1, E_2, E_3 *are (positively proportional to):*

of $\mathbf{e}_1=[1,0,0] \leftrightarrow [0,0]$: *a (in direction of* $\mathbf{e}_1-\mathbf{e}_2$*)*
d (in direction of $\mathbf{e}_1-\mathbf{e}_3$*)*

of $\mathbf{e}_2=[0,1,0] \leftrightarrow [\infty,0]$: $-b$ *(in direction of* $\mathbf{e}_2-\mathbf{e}_1$*)*
$e-b$ *(in direction of* $\mathbf{e}_2-\mathbf{e}_3$*)*

of $\mathbf{e}_3=[0,0,1] \leftrightarrow [0,\infty]$: $-f$ *(in direction of* $\mathbf{e}_3-\mathbf{e}_1$*)*
$c-f$ *(in direction of* $\mathbf{e}_3-\mathbf{e}_2$*).*

Proposition 2. (i) k_1, *respectively,* k_2 *is pointwise fixed under* (2) *iff* $a=b=0$, *respectively,* $d=f=0$.

(ii) *There is an unique fixed point* $[p,0]\in k_1$ *iff* $ab<0$ *and an unique fixed point* $[0,q]\in k_2$ *iff* $df<0$. *In these cases,* $p=-a/b$, $q=-d/f$ *and the* EV's *are of* $[p,0]$: $-a$ *(in direction of* k_1*)*

$$\frac{bd-ae}{b},$$

of $[0,q]$: $-d$ *(in direction of* k_2*)*

$$\frac{af-cd}{f}.$$

(iii) *If neither* (i) *nor* (ii) *happens, no points of* k_1, *respectively,* k_2 *are fixed under* (2).

Corollary 3. *If there is an isolated fixed point* $\lambda\mathbf{e}_i+(1-\lambda)\mathbf{e}_k$, $i\neq k$, $0<\lambda<1$, *under* (1), *then the* EV's *of* $\mathbf{e}_i$ *and* $\mathbf{e}_k$ *in direction* $\mathbf{e}_i-\mathbf{e}_k$ *cannot vanish.*

Corollary 4. *All* EV's *of fixed points on the edges of S are real.*

Proposition 5. (i) *The set* $\{[0, \lambda, 1-\lambda]: 0 \leqq \lambda \leqq 1\}$ *of mixed strategies where* E_1 *is not involved is pointwise fixed under* (1) *iff* $e=b$ *and* $c=f$.

(ii) *There is an unique fixed point* $[0, \lambda, 1-\lambda]$, $0<\lambda<1$, *iff* $(e-b)(f-c)<0$*; in this case,* $\lambda = \frac{c-f}{e-b+c-f}$ *and the* EV's *of* $[0, \lambda, 1-\lambda]$ *are*

$$-\frac{(e-b)(c-f)}{e-b+c-f} \text{ (in direction of } \mathbf{e}_2-\mathbf{e}_3\text{)}$$

and

$$\frac{bf-ce}{e-b+c-f}.$$

(iii) *If neither* (i) *nor* (ii) *happens, no point* $[0, \lambda, 1-\lambda]$, $0<\lambda<1$, *can be fixed under* (1).

Proposition 6. (i) *There is a pointwise fixed straight line g under* (2) *which does not coincide with* k_1 *nor with* k_2 *iff* $bf-ce=ae-bd=cd-af=0$. *In this case,* $g=\{[x,y]: a+bx+cy=0=d+ex+fy\}$.

(ii) *There is an unique fixed point* $[p,q]$, $p>0$, $q>0$, *under* (2), *iff the expressions*

$bf-ce, ae-bd, cd-af$

all have the same sign $\neq 0$. *In this case,* $p=\frac{cd-af}{bf-ce}$, $q=\frac{ae-bd}{bf-ce}$ *and the* EV's *of* $[p,q]$ *are* $\lambda_{1,2}=\frac{1}{2}(bp+fq \pm \sqrt{(bp+fq)^2-4pq(bf-ce)})$.

(iii) *If neither* (i) *nor* (ii) *is the case, there is no fixed point* $[p,q]$, $p>0$, $q>0$, *under* (2).

Corollary 7. *If* $[p,q]$, $p>0, q>0$, *is an isolated fixed point (situation* (ii) *in Proposition* 6*) with* EV's $\lambda_{1,2}$ *then*

(i) $\lambda_{1,2} \neq 0$.

(ii) $bf<ce$ *iff* $\lambda_1<0<\lambda_2$ *iff* $[p,q]$ *is a hyperbolic saddle point.*

(iii) $bf>ce$ *iff the real parts of* $\lambda_{1,2}$ *have the same sign as* $bp+fq$*; hence*

(iiia) $bp+fq>0$ *iff* $[p,q]$ *is a hyperbolic source.*

(iiib) $bp+fq=0$ *iff* $\lambda_1=\bar{\lambda}_2 \neq 0$; $[p,q]$ *is a "centre".*

(iiic) $bp+fq<0$ *iff* $[p,q]$ *is a hyperbolic sink.*

Corollary 8. *Let* $[p,q]$, $p>0$, $q>0$, *be an isolated fixed point; then*

(i) *each vertex* $\mathbf{e}_1$, $\mathbf{e}_2$, $\mathbf{e}_3$ *has at least one* EV *which does not vanish;*

(ii) *if there is a non-corner fixed point on an edge, it must be isolated and all its* EV's *do not vanish.*

Proposition 9. *If there are two different pointwise fixed straight lines under* (2) *which do not coincide with* k_1 *nor with* k_2 *then* $A=[0]$.

Remark. The statements (iii) in Propositions 2, 5, and 6 and that in Proposition 9 can be deduced from the following fact: if two mixed strategies with the same pure strategies involved are fixed then the straight line joining them is already pointwise fixed; this is an important property of the dynamics (1) and (2) which is easily verified.

References

Akin, E., Hofbauer, J.: Recurrence of the unfit. Math. Biosci. **61**, 51–63 (1982)

Eigen, M., Schuster, P.: The hypercycle – a principle of natural selforganization. Berlin, Heidelberg, New York: Springer 1979

Hadeler, K.: Mathematik für Biologen. In: Heidelberger Taschenbuch, Bd. 129. Berlin, Heidelberg, New York: Springer 1974

Hofbauer, J., Schuster, P., Sigmund, K.: A note on evolutionary stable strategies and game dynamics. J. Theor. Biol. **81**, 609–612 (1979)

Hofbauer, J.: On the occurrence of limit cycles in the Volterra-Lotka differential equation. J. Nonlinear Anal. **5**, 1003–1007 (1981)

Li, L.C.: Unpublished notes. Cornell University (1979)

Maynard-Smith, J., Price, G.R.: The logic of animal conflict. Nature (London) **246**, 15–18 (1973)

Maynard-Smith, J.: The theory of games and the evolution of animal conflicts. J. Theor. Biol. **47**, 209–221 (1974)

Maynard-Smith, J.: Evolution and the theory of games. Cambridge: Cambridge University Press 1982

Schuster, P., Sigmund, K., Wolff, R.: Mass action kinetics of selfreplication in flow reactors. J. Math. Anal. Appl. **78**, 88–112 (1980)

Schuster, P., Sigmund, K., Hofbauer, J., Wolff, R.: Selfregulation of behaviour in animal societies. Biol. Cybern. **40**, 1–8 (1981)

Schuster, P., Sigmund, K.: Replicator dynamics. J. Theor. Biol. **100**, 533–538 (1983)

Taylor, P., Jonker, L.: Evolutionarily stable strategies and game dynamics. Math. Biosci. **40**, 145–156 (1978)

Zeeman, E.C.: Population dynamics from game theory. In: Lecture Notes in Mathematics, Vol. 819. Global theory of dynamical systems. Nitecki, Z., Robinson, C. (eds.). Berlin, Heidelberg, New York: Springer 1980

Zeeman, E.C.: Dynamics of the evolution of animal conflicts. J. Theor. Biol. **89**, 249–270 (1981)

Received: July 4, 1983

Dr. Immanuel M. Bomze
Institut für Statistik und Informatik
der Universität Wien
Rathausstrasse 19
A-1010 Wien
Austria